Impacts of Anthropogenic Heat on Summertime Rainfall in Beijing

Wanshu Nie[1,2]*, Benjamin F. Zaitchik[1], Guangheng Ni[2], Ting Sun[2]

[1]Department of Earth and Planetary Science, The Johns Hopkins University, Baltimore, Maryland

[2]State Key Laboratory of Hydro-Science and Engineering, Department of Hydraulic Engineering, Tsinghua University, Beijing, China

*Email: nwanshu1@jhu.edu

Introduction

Anthropogenic heat (AH) is an important component of the urban energy budgets that can affect land surface and atmospheric boundary layer processes. Representation of anthropogenic heat in numerical climate modeling systems is, therefore, important when simulating urban meteorology and climate, and has the potential to improve weather forecasts, climate process studies, and energy demand analysis.

Our **objective** is to study the sensitivity of simulated precipitation to AH, to evaluate the impact that AH has on model performance relative to available observations, and to investigate mechanisms through which AH influences the convective environment.

WRF-UCM-BEM Experiment

We incorporate spatiotemporally dynamic anthropogenic heat data estimated by the Building Effects Parameterization and Building Energy Model (**BEP-BEM**) into the Weather Research and Forecasting system (**WRF**) to investigate its impact on simulation of summertime rainfall in Beijing, China.

Four summertime local rainfall events are selected and simulations are conducted with and without anthropogenic heat.

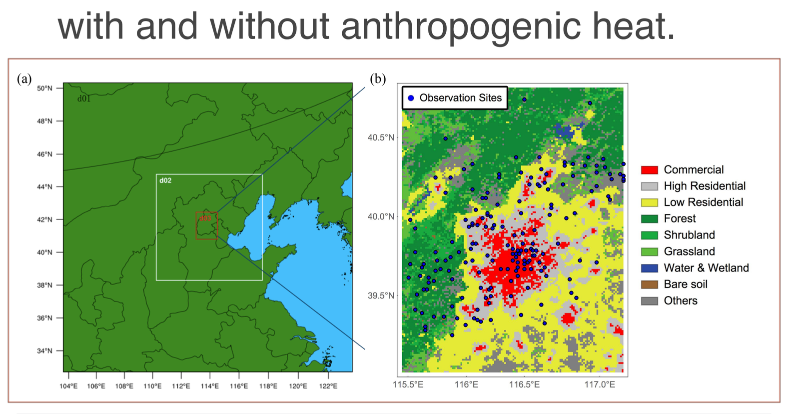

Fig.1 WRF simulation configuration of (a) one-way nested domains and (b) the land cover map for the innermost domain (D03).

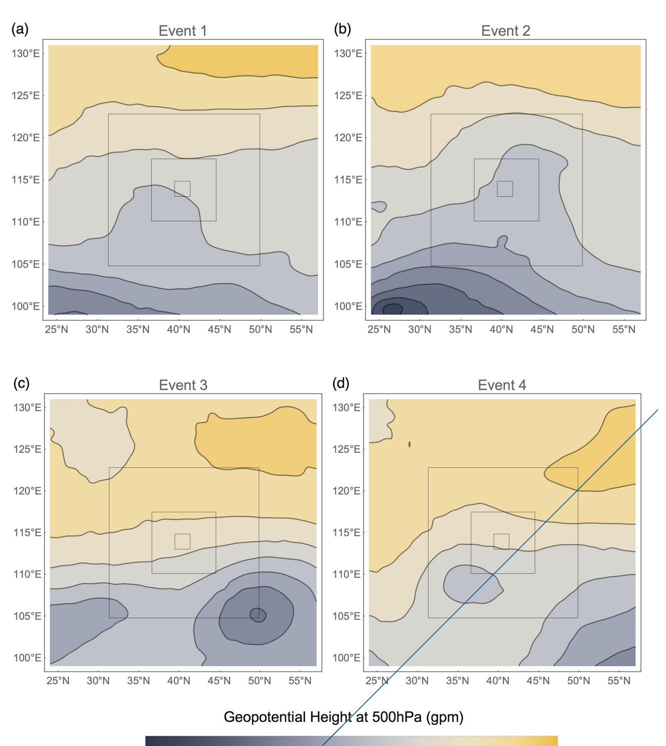

Fig.2 The synoptic weather pattern of geopotential height at 500 hPa for (a) 0800 LT 1 Jul 2014, (b) 1400 LT 2 Jul 2014, (c) 1400 LT 27 Jul 2015 and (d) 1400 LT 29 Jul 2015.

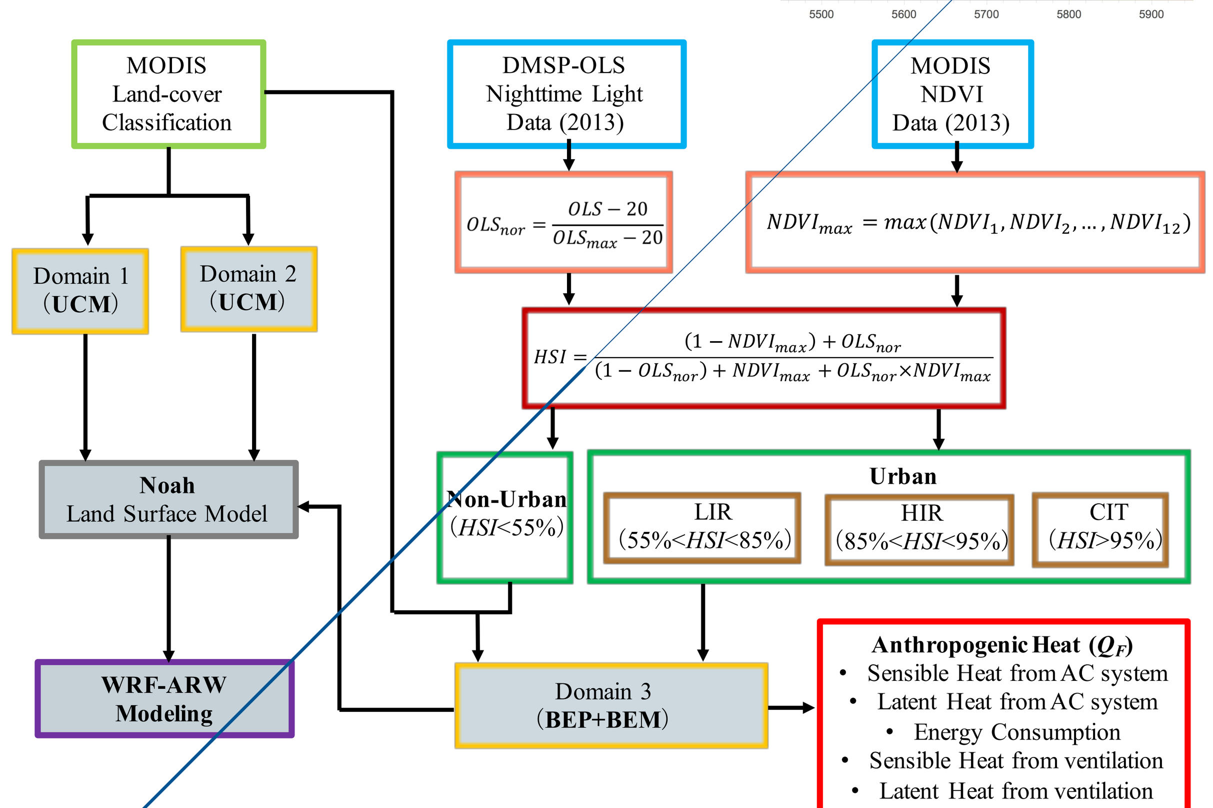

Fig.3 Flow chart for updating the land cover map based on DMSP-OLS nighttime light data and MODIS NDVI data and estimating AH in BEP-BEM.

Results and Discussion

1. AH Spatiotemporal pattern

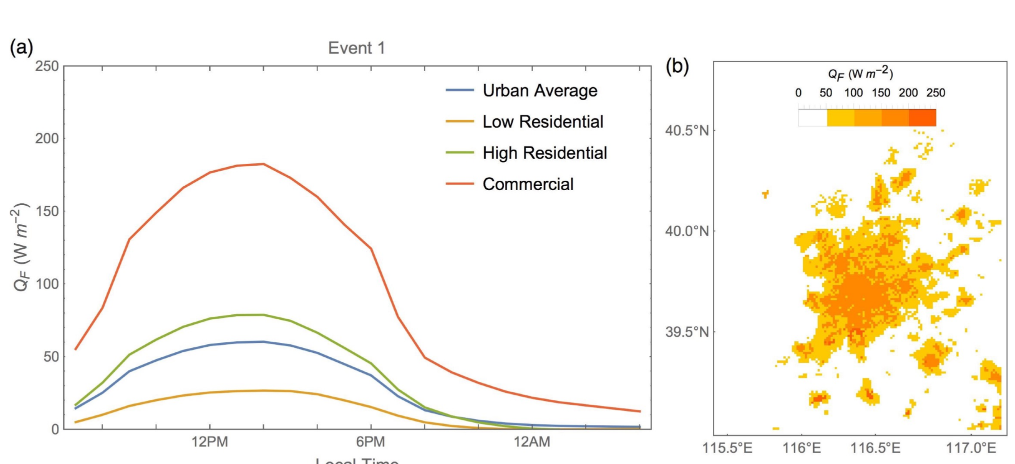

Fig.4 (a) spatially averaged diurnal cycle in AH_{ON} for each urban land cover class and for the all-urban average and (b) peak hour AH map for event 1.

- The area of higher building density has higher AH values.
- The peak of AH appears in the late afternoon, reflecting the timing of maximum air-conditioning loads.

2. Urban Energy Balance

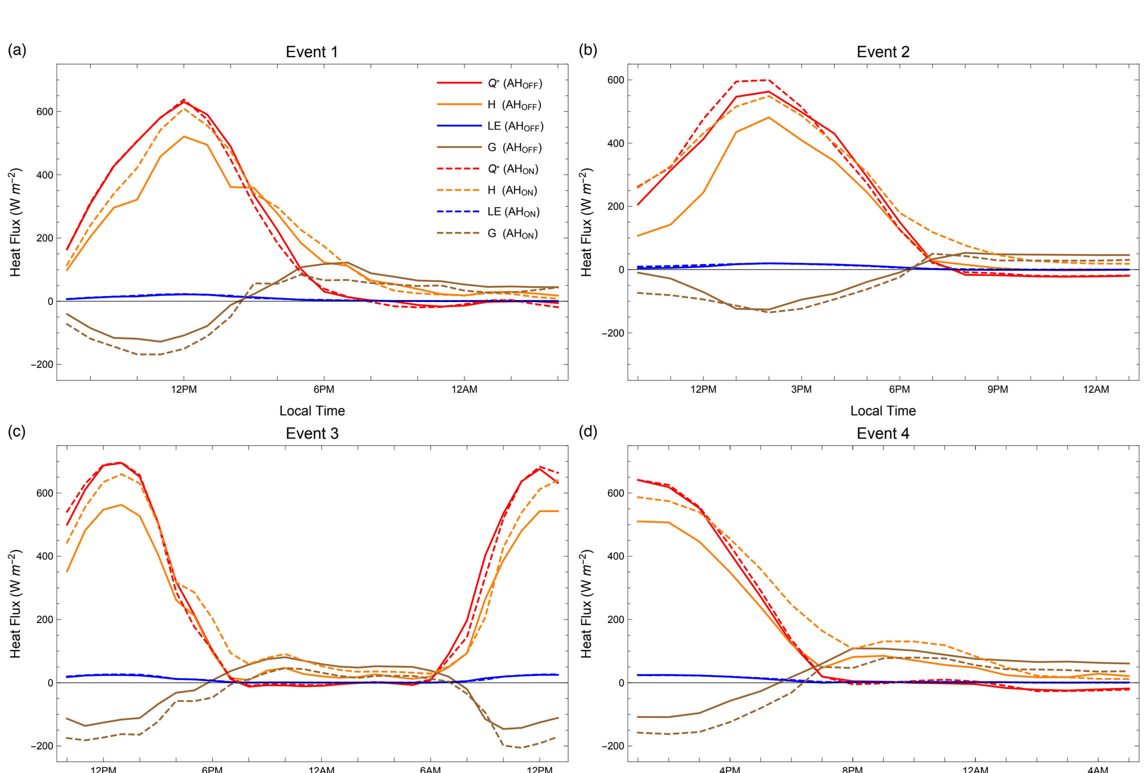

Fig.5 Temporal profile of urban averaged sensible heat, latent heat and ground heat fluxes for each event in AH_{ON} and AH_{OFF}.

- AH influence on the atmosphere is primarily via **sensible heat**.
- The peak area of sensible heat increase is located in the commercial area, which is consistent with the spatial pattern of AH.

3. Atmospheric boundary layer

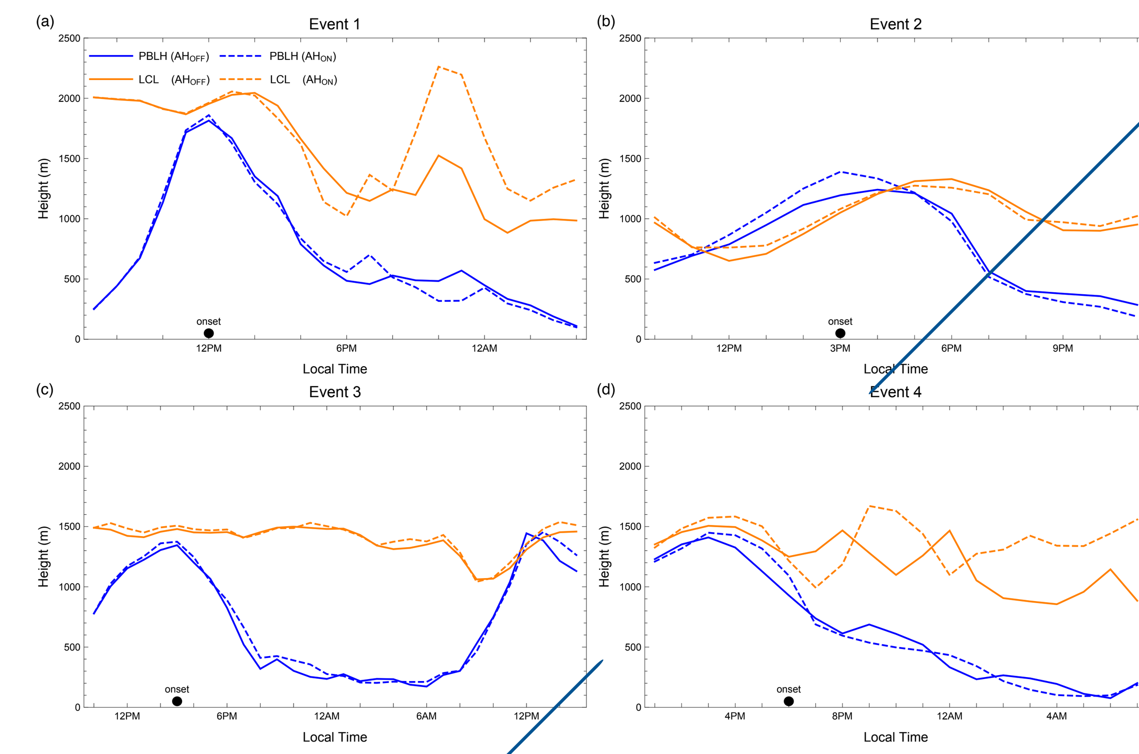

- Urban averaged **PBL heights** in the pre-storm period in AH_{ON} are systematically greater than AH_{OFF}.
- Greater atmospheric dry-down and a higher post-event **LCL** are found in AH_{ON}.
- AH impacts on pre-storm MSE density within PBL are negligible, as the contribution of AH to thermal energy (c_pT) is approximately counterbalanced by the deepening of the PBL and associated entrainment of lower energy air from the free troposphere.

Fig.6 Temporal profile of urban averaged PBL height and LCL in AH_{ON} and AH_{OFF} for each event.

4. Atmospheric stability

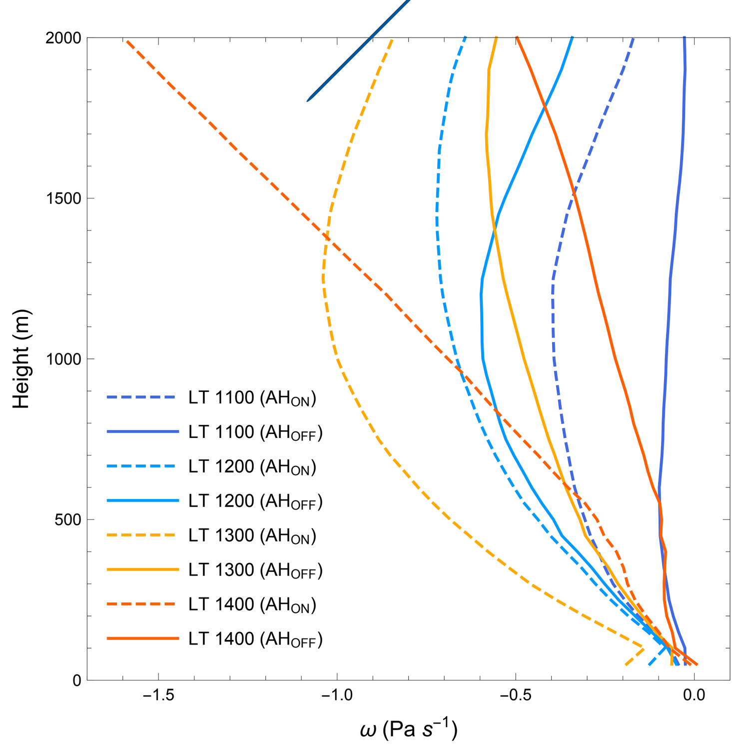

Fig.7 Pressure velocity (ω) for 1100-1400 LT in the commercial area for event 1.

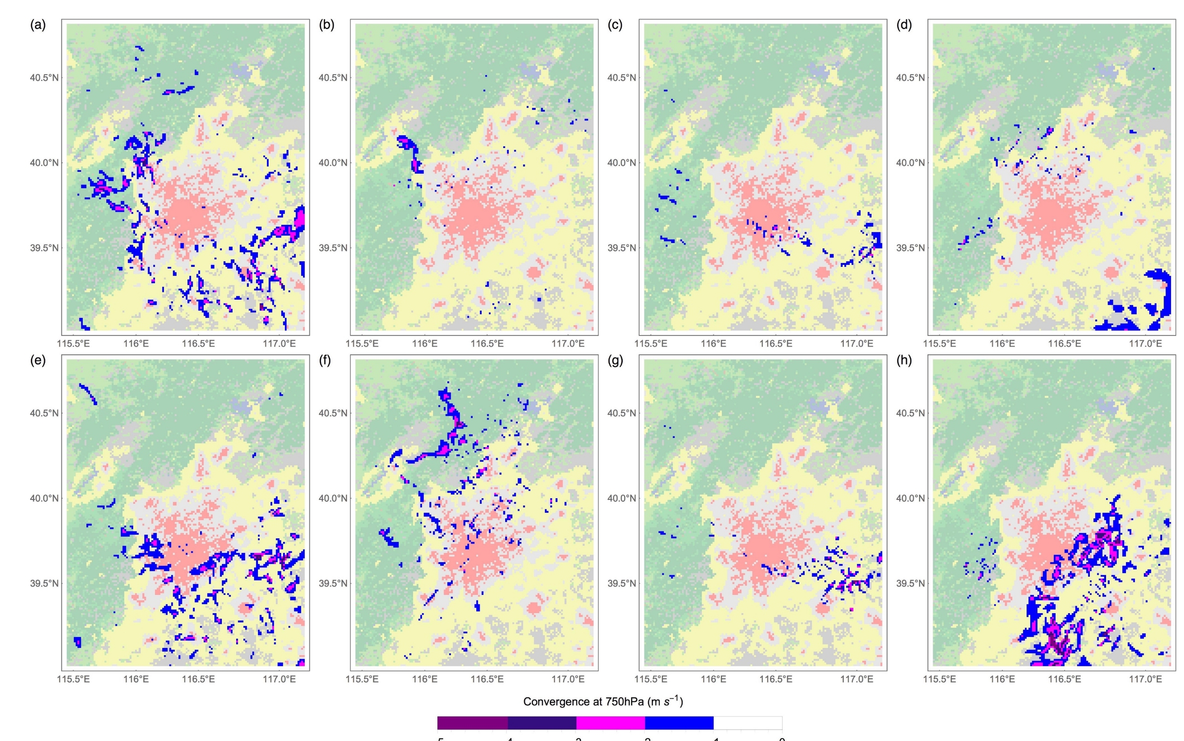

Fig.8 Low-level convergence at 750 hPa during the convective period for each event in AH_{OFF} at (a) 1800 LT, (b) 1900 LT, (c) 2200 LT, (d) 2300 LT and in AH_{ON} at (e) 1800 LT, (f) 1900 LT, (g) 2200 LT, (h) 2300 LT.

- Stronger **upward motion** before the onset of precipitation.
- Enhanced **convergence** due to AH are more likely to generate over the interface of three urban land covers and urban-rural borders possibly due to the flux gradients.

5. Cumulative Rainfall

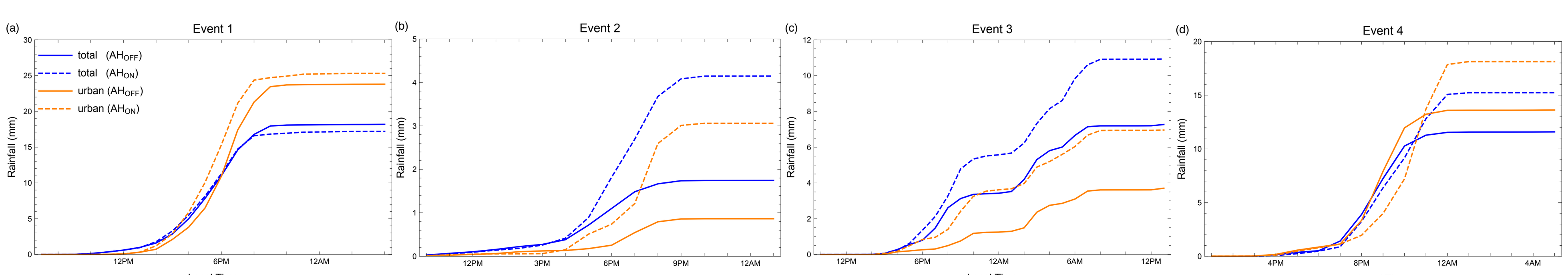

Fig.9 Urban averaged and domain 3 (D03) averaged cumulative rainfall in AH_{ON} and AH_{OFF} for each event.

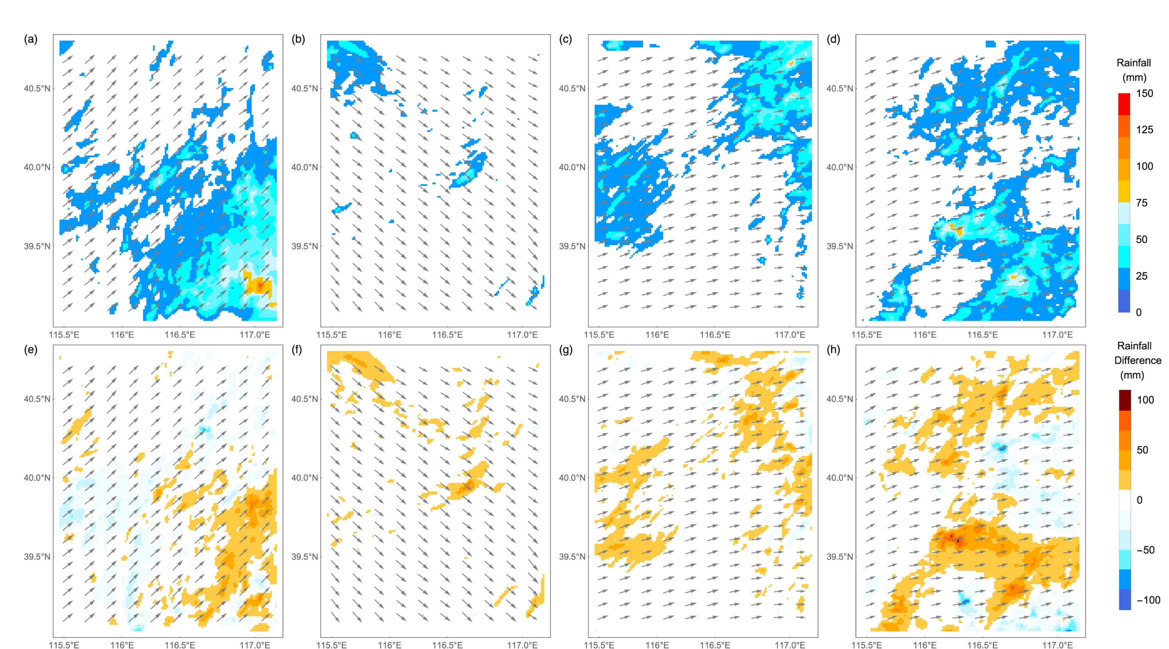

AH increases rainfall in the urban area and surroundings. However, it influences rainfall through **multiple mechanisms**. In event 1 and 3, AH causes the PBL to deepen to the LCL faster in AH_{ON} than AH_{OFF} there can be an earlier onset of rainfall, while in event 2 and 4, entrainment at the top of the PBL can delay the onset of rain, but destabilization of the lower atmosphere due to AH eventually leads to more total rainfall.

Fig.10 Spatial distribution of cumulative rainfall and horizontal background wind speed at 500 hPa for (a) event 1, (b) event 2, (c) event 3, (d) event 4 in AH_{ON} and its difference compared to AH_{OFF} for (e) event 1, (f) event 2, (g) event 3, (h) event 4.

Conclusion

Acknowledgement /

National Natural Science Foundation of China 51190092
National Natural Science Foundation of China 51409147
China Postdoctoral Science Foundation 2015T80093

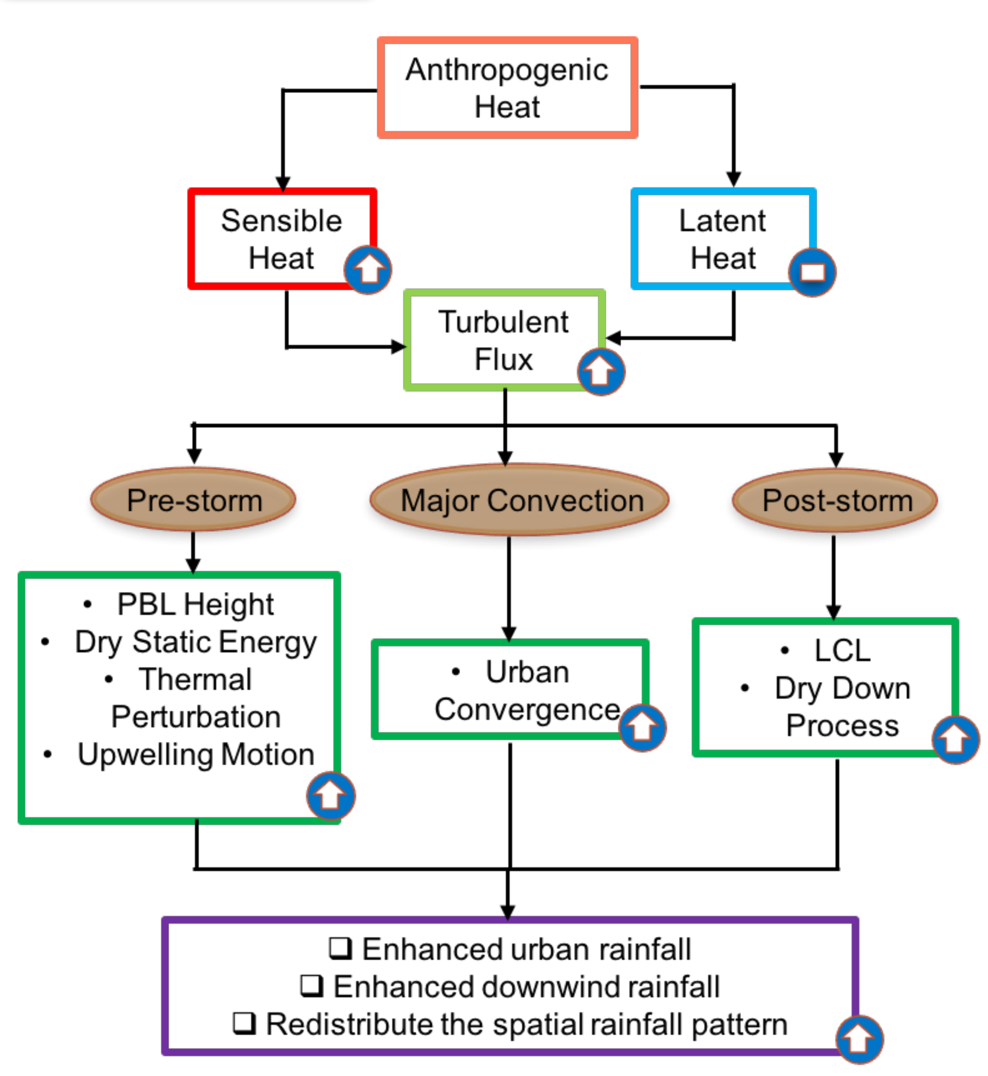

Anthropogenic heat emission increases sensible heat flux, enhances mixing and turbulent energy transport, lifts PBL height, increases dry static energy and destabilizes the atmosphere in urban areas through thermal perturbation and strong upwelling motion during the pre-storm period, resulting in enhanced convergence during the major rainfall period. Intensified rainfall leads to greater atmospheric dry-down during the storm and a higher post-storm LCL.

References

1. Chen, F., X. Yang, and J. Wu, 2016: Simulation of the urban climate in a Chinese megacity with spatially heterogeneous anthropogenic heat data. *Journal of Geophysical Research: Atmospheres.*

2. Lu, D., H. Tian, G. Zhou, and H. Ge, 2008: Regional mapping of human settlements in southeastern China with multisensor remotely sensed data. *Remote Sensing of Environment*, **112,** 3668-3679.

3. Shepherd, J. M., 2005: A review of current investigations of urban-induced rainfall and recommendations for the future. *Earth Interactions*, **9**, 1-27.